Article

Morphological and Immunohistochemical Features of Secondary Immune Organs (Regional Lymph Nodes and Spleen) in Acute Secondary Peritonitis

Azizjon K.Khaydarov *[1], **Erkin E.Eshbaev** [2]

[1] Department of Traumatology and Orthopedics, Fergana Medical Institute of Public Health, Fergana, 150100, Uzbekistan
[2] Department of Pathological Anatomy, Tashkent State Medical University, Tashkent, 100109, Uzbekistan
haydarov.azizjon@mail.ru (A.Kh.), dr.erkin.eshbayev@gmail.com (E.E.)
* Correspondence: haydarov.azizjon@mail.ru; Tel.: +998 88 3634446 (A.Kh.)

Abstract:

Aim. To characterize morphological and immunohistochemical (IHC) features of mesenteric lymph nodes and spleen in fatal acute secondary peritonitis, using age-matched non-septic tissue as a qualitative reference.

Materials and Methods. Autopsy-based cross-sectional study at the Republican Pathological Anatomy Center (2018–2023). Mesenteric lymph nodes and spleen were examined from 131 adults (18–45 years) who died of acute secondary peritonitis, alongside 15 age-matched non-septic controls (acute myocardial infarction, no systemic inflammation) that served as a qualitative reference. Specimens were fixed in 10% buffered formalin, embedded in paraffin, and stained with hematoxylin-eosin (H&E); 33 lymph node specimens underwent IHC for CD3, CD4, CD20 and CD68, and 32 spleen specimens for CD8, CD68 and Ki-67, with DAB detection. Results are expressed as counts, percentages with 95% confidence intervals (Wilson score method), or mean ± standard deviation (M±SD).

Results. Within 24–72 hours, both organs showed secondary lymphoid collapse: germinal-center depletion, marginal-zone denudation, T- and B-lymphocyte migration toward inflamed foci, reticulocyte and macrophage proliferation, and interstitial edema. In lymph nodes, CD68 macrophage positivity occurred in 27/33 cases (81.8%; 95% CI 65.6–91.4%); CD3/CD4 T-lymphocytes were low/absent in 21/33 (63.6%) and 12/33 (36.4%) cases; CD20 B-lymphocytes were reduced/absent in 32/33 (97.0%). In spleen, CD8 T-lymphocyte depletion was moderately positive in 27/32 cases (84.4%; 95% CI 68.2–93.1%); Ki-67 proliferation index was 16.21 ± 1.06%, indicating insufficient regeneration.

Conclusion. Acute secondary peritonitis produces time-dependent structural and immunophenotypic collapse in lymph nodes and spleen, with T- and B-lymphocyte depletion and compensatory macrophage hyperplasia.

Keyword: acute secondary peritonitis, mesenteric lymph node, spleen, immunohistochemistry, CD3, CD4, CD8, CD20, CD68, Ki-67, secondary immunodeficiency.

Quoting: Azizjon K.Khaydarov, Erkin E.Eshbaev. Morphological and Immunohistochemical Features of Secondary Immune Organs in Acute Secondary Peritonitis. **2026**, 5, 3, 3. https://doi.org/10.56121/MSU-2026-3-00015

Received: 26.03.2026
Corrected: 19.04.2026
Accepted: 20.05.2026
Published: 29.06.2026

Introduction

Acute peritonitis remains one of the most lethal conditions in emergency abdominal surgery, with case-fatality rates reported in the 20–60% range worldwide [1,2]; regional registry data cited in the authors' preceding dissertation materials suggest still higher lethality (up to 60–85%) in some Central Asian cohorts, a figure that awaits independent confirmation in the peer-reviewed literature. The clinical course is largely determined not only by the primary abdominal source but by the systemic response of the immune system: overwhelming activation of peripheral secondary immune organs — chiefly the regional (mesenteric) lymph nodes, the spleen, and gut-associated lymphoid tissue (MALT) — followed by their functional collapse, a cytokine-mediated systemic inflammatory response, and progression to sepsis, septic shock and multiple organ dysfunction [3–5].

Regional mesenteric lymph nodes are the first anatomical barrier draining the peritoneal cavity; loss of their drainage and filtration capacity allows uncontrolled hematogenous and lymphogenous

spread of bacterial products, precipitating septicemia and septicopyemia. The spleen, as the largest peripheral lymphoid organ, mounts a parallel but distinct response, dominated by follicular marginal-zone denudation, germinal-center B-lymphocyte loss, red-pulp congestion and erythrocyte hemolysis. Despite the clinical importance of this axis, the morphological and immunohistochemical substrate of secondary immune organ failure in adult acute secondary peritonitis has not been systematically characterized, and no quantitative immunophenotypic criteria currently exist to grade its severity.

The aim of this study was to characterize, in a defined cohort of adults (18–45 years) who died of acute secondary peritonitis, the morphological and immunohistochemical (CD3, CD4, CD20 and CD68 in mesenteric lymph nodes; CD8, CD68 and Ki-67 in spleen) features of these organs, using the findings in age-matched non-septic controls as a qualitative reference state.

Materials and Methods

Study design and material

This was a retrospective, autopsy-based, cross-sectional comparative morphological study conducted on material from the Republican Pathological Anatomy Center and its Fergana branch, covering the period 2018–2023. The study group comprised 131 deceased adults, aged 18–45 years, with a confirmed intraoperative and autopsy diagnosis of acute secondary peritonitis of surgical (predominantly gastrointestinal and biliary) origin; the reported 24–72-hour interval refers to the time elapsed from the intraoperatively documented onset of diffuse peritonitis to death/autopsy in each case. The control group comprised 15 age-matched individuals who died of acute myocardial infarction, without clinical or morphological evidence of peritonitis, sepsis, or other systemic inflammatory or immunological disease; on H&E and IHC screening, their mesenteric lymph nodes and splenic tissue showed preserved germinal-center architecture, an intact marginal zone, and normal paracortical/periarteriolar T- and follicular B-lymphocyte density, serving as the qualitative reference state against which the peritonitis-group findings below are described. Formal quantitative comparison between the two groups (with control-group n (%)/M$\pm$SD data) is reported separately, as detailed under Statistical analysis below.

subsectionTissue processing

Mesenteric lymph nodes (from the ileocecal drainage territory) and spleen tissue were sampled at autopsy, fixed in 10% neutral buffered formalin, routinely processed and embedded in paraffin. Serial sections of 4–5 μm were stained with hematoxylin and eosin (H&E) for baseline morphological evaluation in all cases.

Immunohistochemistry

A representative subset of cases underwent IHC staining, selected consecutively from the parent cohort on the basis of adequate paraffin-block tissue preservation and availability of sufficient serial sections for the applicable antibody panel: 33 mesenteric lymph node specimens and 32 spleen specimens met these criteria and were included. Sections were stained using the streptavidin-biotin/DAB chromogen method with an organ-specific primary antibody panel, selected to characterize the cellular compartments most relevant to each organ's response: mesenteric lymph node specimens were stained for CD3 and CD4 (pan-T and helper-T lymphocyte markers, assessed jointly as a combined paracortical T-lymphocyte panel), CD20 (B-lymphocyte marker) and CD68 (macrophage/histiocyte marker); spleen specimens were stained for CD8 (cytotoxic/suppressor T-lymphocyte marker), CD68 (macrophage/histiocyte marker) and Ki-67 (nuclear proliferation marker). Nuclei were counterstained with hematoxylin. Immunoreactivity was graded semi-quantitatively by two independent observers as negative, low-positive, or moderate/high-positive, based on the proportion and intensity of stained cells within representative high-power fields; the Ki-67 proliferation (mitotic) index was calculated as the percentage of Ki-67-positive nuclei among lymphoblastic cells counted across five random high-power fields ($\times$20).

Microscopy and imaging

All sections were examined under an Olympus-series light microscope at magnifications of $\times$40 to $\times$400 (objective $\times$4–$\times$40, eyepiece $\times$10). Representative fields were digitally photographed with an integrated microscope camera; scale bars are shown on the original micrographs where captured by the imaging software.

Statistical analysis

Categorical IHC findings (positive/negative, and low/moderate/high positivity) are presented as absolute counts and percentages of the examined subset, with 95% confidence intervals calculated by the Wilson score method. The Ki-67 proliferation index is expressed as mean ± standard deviation (M±SD) of the percentage of Ki-67-positive nuclei per high-power field, calculated across five replicate fields (×20) per specimen. Because of the descriptive, single-cohort design of the present communication, formal between-group inferential testing (e.g., χ^2, Student's t-test) was not performed; such comparison against the non-septic control group is the subject of the authors' ongoing dissertation research and will be reported separately with full case-by-case data.

Ethics statement

The study was approved by the scientific and ethics committee of the Fergana Medical Institute of Public Health, protocol No. K/2025 0BB1, December 2025. As an autopsy-based archival material study, individual patient consent for the underlying clinical care was not applicable; all material was anonymized prior to analysis, and the study was conducted in accordance with the Declaration of Helsinki principles for research using post-mortem human tissue.

Results

Morphology of the mesenteric lymph nodes

Within the first 24–72 hours of acute secondary peritonitis, mesenteric lymph nodes showed a consistent sequence of reactive-to-exhaustive changes. Early lesions were dominated by capsular tension, subcapsular sinus dilation filled with proteinaceous (eosinophilic, homogeneous) exudate, and massive vascular congestion of the hilar and cortical vessels (Figure 1). Marked lymphocyte depletion was evident in both the cortical (B-cell) and paracortical (T-cell) zones, with secondary follicles showing 'naked', depopulated germinal centers and loss of normal follicular texture.

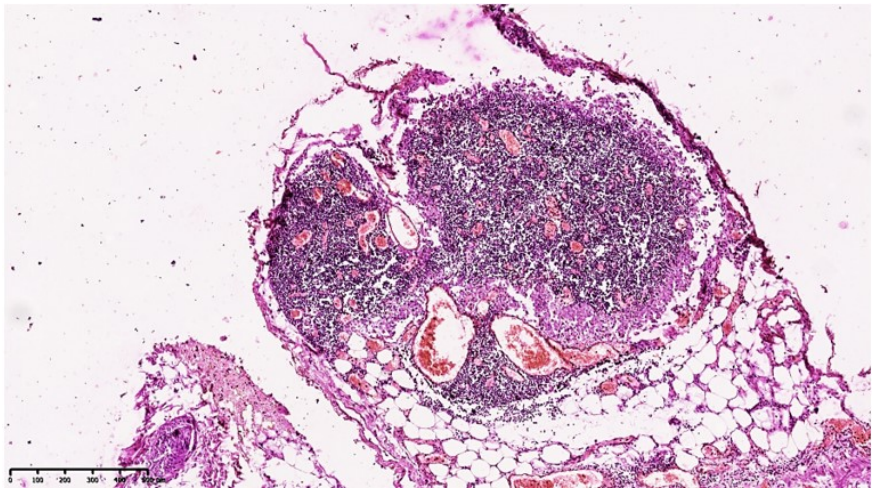

Figure 1. Mesenteric lymph node, acute secondary peritonitis. Low-power view showing marked congestion of hilar and cortical vessels, diffuse depletion of cortical lymphocytes, and subcapsular deposition of homogeneous eosinophilic (proteinaceous) material. H&E, ×40–100.

At higher magnification, the paracortical and medullary cords showed a striking shift in cellular composition: small lymphocytes were replaced by numerous macrophages, reticular cells, and scattered fibroblasts, with interstitial edema and dispersed cellular debris. Macrophages were frequently enlarged, with coarse basophilic cytoplasmic inclusions consistent with active phagocytosis of tissue fragments (Figure 2). Mast-cell numbers were increased in the medullary sinuses, and foci of degranulation were noted, a pattern that may suggest an accompanying local cytokine-release response, although cytokine levels were not directly measured in this study.

Morphology of the spleen

Splenic tissue in the peritonitis group showed variable-degree follicular hyperplasia together with severe marginal-zone denudation of the white-pulp lymphoid follicles: the B-lymphocyte/T-lymphocyte mixture of the marginal zone was sharply reduced, and the T-lymphocyte cuff surrounding the central (follicular) artery was likewise depleted, leaving a 'naked', stroma-only appearance that

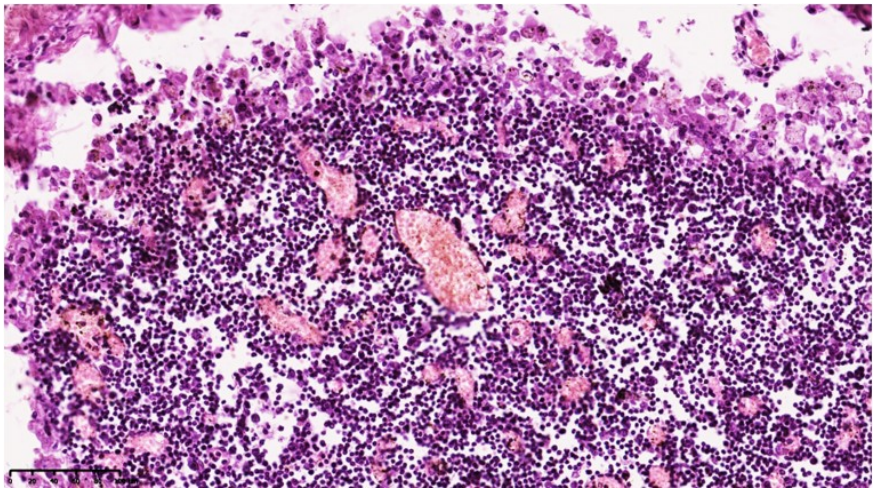

Figure 2. Mesenteric lymph node. Medullary region showing dense accumulation of macrophages and reticular cells with sharply reduced numbers of residual lymphocytes; scattered proteinaceous deposits and erythrocyte extravasation are present. H&E, ×200–400.

the authors' original material likened to a 'setting sun' pattern around the follicle margin (Figure 3). Red-pulp changes were dominated by pronounced congestion and dilation of the pulp veins, increased erythrocyte hemolysis, and accumulation of siderophages, particularly around the perimeter of the Billroth cords.

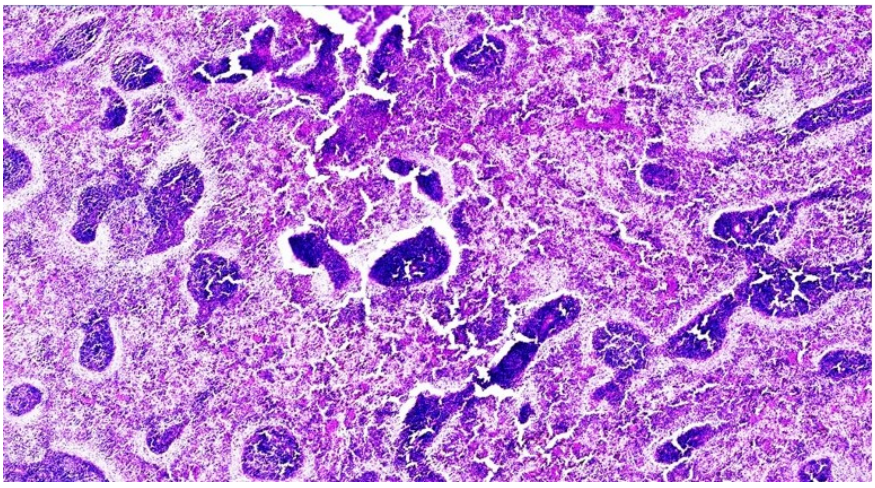

Figure 3. Spleen, acute secondary peritonitis. White-pulp lymphoid follicles with marked marginal-zone denudation and germinal-center depletion; red-pulp congestion is visible at the periphery. H&E, ×40–100.

Subcapsular and perifollicular regions frequently contained coarse, homogeneous eosinophilic protein deposits, interpreted as drained inflammatory exudate components and immune-complex substrate, analogous to the deposits observed in lymph nodes. Trabecular vessels showed marked dilation with surrounding reticulocytosis. Overall, the combination of follicular collapse, red-pulp hemolysis and stromal protein deposition is consistent with acute functional impairment of splenic immune surveillance during the earliest phase of peritonitis, though this morphological interpretation was not corroborated by direct functional assays.

Immunohistochemical findings — mesenteric lymph nodes

IHC staining of 33 lymph node specimens confirmed and quantified the morphological impression of combined T- and B-lymphocyte depletion with compensatory macrophage expansion. CD68-positive macrophages, morphologically enlarged with coarse cytoplasmic granularity, showed moderate-to-high positive expression in 27/33 cases (81.8%; 95% CI 65.6–91.4%) and low-positive

expression in the remaining 6/33 cases (18.2%), with macrophage accumulation concentrated in the paracortical cords and around collapsed germinal centers (Figure 4).

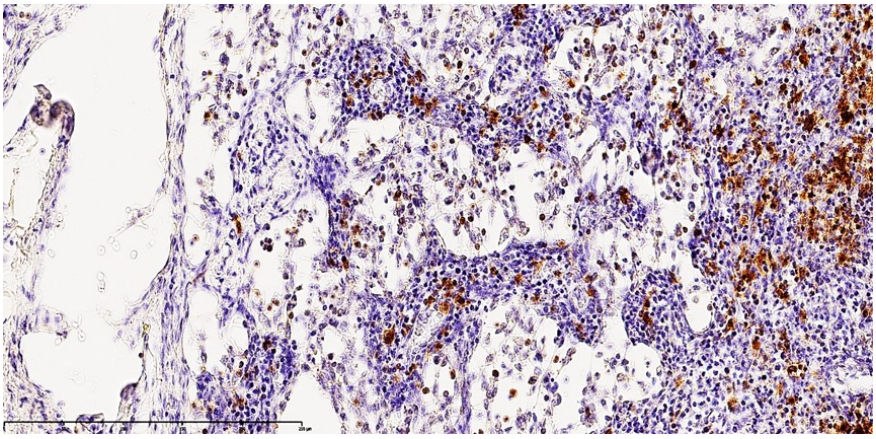

Figure 4. Mesenteric lymph node, acute secondary peritonitis. CD68 immunostaining showing clusters of strongly positive macrophages (brown) within the paracortical region, corresponding to sites of germinal-center collapse. DAB chromogen, ×100–200.

In contrast, paracortical CD3- and CD4-positive T-lymphocytes — evaluated jointly as a combined pan-T/helper-T panel rather than as separately quantified markers in the present cohort — showed low-positive reactivity in 21/33 cases (63.6%) and were essentially negative in 12/33 cases (36.4%), indicating pronounced T-cell depletion consistent with acute cellular immunodeficiency; marker-specific (CD3 vs. CD4) case-by-case quantification is planned for the authors' subsequent comparative report. CD20-positive B-lymphocytes were even more severely affected: moderate-to-low positive expression was observed in only 11/33 cases (33.3%), while 21/33 cases (63.6%) were frankly negative, confirming near-complete collapse of the follicular B-cell compartment. Taken together, these findings indicate that, within the first 24–72 hours of acute peritonitis, mesenteric lymph nodes undergo massive antigen-dependent lymphocyte mobilization toward inflamed foci, leaving behind a reticulocyte- and macrophage-rich, lymphocyte-depleted stroma — the morphological substrate of secondary lymph-node immunodeficiency.

Immunohistochemical findings — spleen

Among 32 spleen specimens examined by IHC, CD8-positive cytotoxic/suppressor T-lymphocytes around the periarteriolar lymphoid sheath showed moderate positive expression in 27/32 cases (84.4%; 95% CI 68.2–93.1%) and negative reactivity in 5/32 cases (15.6%); however, the positive cells were predominantly small, poorly differentiated lymphoblasts rather than mature effector T-cells, a pattern that may suggest incomplete antigen-dependent differentiation (Figure 5).

Ki-67 nuclear staining, performed to assess the proliferative response of the depleted lymphoid compartment, showed moderate-to-high positive expression predominantly in residual lymphoblasts and occasional macrophages, most concentrated at the follicular margins and periarteriolar T-zone. The calculated proliferation (mitotic) index was 16.21 ± 1.06% (M±SD), consistent with a compensatory but quantitatively insufficient regenerative attempt against ongoing lymphocyte loss.

CD68 staining of splenic macrophages showed a pattern distinct from that in the lymph nodes: positive cells were relatively sparse and diffusely distributed through red and white pulp, frequently in a hemosiderin-laden (siderophage) form, in 21/32 cases (65.6%) with moderate positivity, 8/32 cases (25.0%) low-positive, and 3/32 cases (9.4%) negative (Figure 6). This comparatively reduced and slowed macrophage/phagocytic response — in contrast to the pronounced macrophage hyperplasia seen in lymph nodes — suggests that splenic clearance of toxic metabolites and cellular debris lags behind the lymph-node response during the earliest (24–72 hour) phase of peritonitis, a finding with direct relevance to the pace of systemic toxin elimination in early sepsis.

Summary of quantitative immunohistochemical findings

Table 1 summarizes the semi-quantitative IHC expression patterns across both organs. The consistent pattern — pronounced T- and B-lymphocyte depletion with compensatory but qualitatively immature (macrophage/lymphoblast-dominated) cellular repopulation — was observed in both the

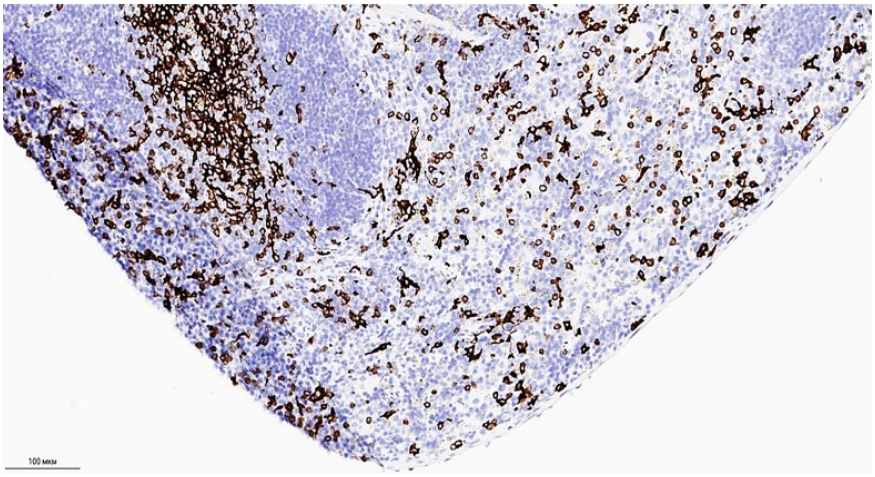

Figure 5. Spleen, acute secondary peritonitis. CD8 immunostaining of the periarteriolar lymphoid sheath, showing scattered positive lymphoblast-like cells with loss of the normal dense T-cell cuff around the central artery. DAB chromogen, ×200.

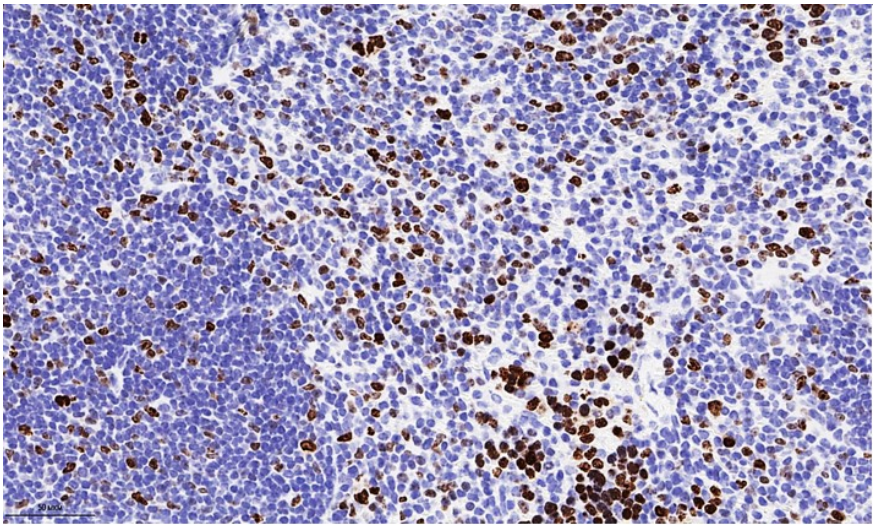

Figure 6. Spleen, acute secondary peritonitis. CD68 immunostaining showing scattered, predominantly hemosiderin-laden macrophages (siderophages) within the red pulp and marginal zone, with comparatively sparse distribution relative to the lymph-node macrophage response. DAB chromogen, ×200.

regional lymph nodes and the spleen, supporting a unified concept of acute secondary peripheral immune organ collapse in severe peritonitis.

Discussion:

The present findings demonstrate that acute secondary peritonitis triggers a rapid, coordinated structural and immunophenotypic collapse of both principal peripheral secondary immune organs — the mesenteric lymph nodes and the spleen — within the first 24–72 hours of disease onset. This pattern is characterized by three convergent processes: (i) massive, antigen-dependent mobilization of mature T- and B-lymphocytes out of the organized lymphoid compartments (germinal centers, paracortex, periarteriolar lymphoid sheath) toward inflamed peritoneal foci; (ii) compensatory but qualitatively immature repopulation of the depleted stroma by macrophages, reticular cells and lymphoblasts, reflected in elevated CD68 positivity and a Ki-67 proliferation index of 16.21 $\pm$ 1.06%; and (iii) organ-specific secondary changes — interstitial edema and delimfatization in lymph nodes, and red-pulp congestion with erythrocyte hemolysis and siderophage accumulation in the spleen.

Table 1. Semi-Fimmunohistochemical expression of lymphocyte and macrophage markers in mesenteric lymph nodes and spleen in acute secondary peritonitis.

Organ	Marker	n examined	Moderate/high positive, n (%)	Low positive, n (%)	Negative, n (%)
Mesenteric lymph node	CD68 (macrophages)	33	27 (81.8)	6 (18.2)	0 (0.0)
Mesenteric lymph node	CD3 / CD4 (T-cells, combined panel)	33	0 (0.0)	21 (63.6)	12 (36.4)
Mesenteric lymph node	CD20 (B-cells)	33	0 (0.0)	11 (33.3)	21 (63.6)*
Spleen	CD8 (T-cells, PALS)	32	27 (84.4)	0 (0.0)	5 (15.6)
Spleen	CD68 (macrophages)	32	21 (65.6)	8 (25.0)	3 (9.4)

* Values are n (%) of examined specimens; 95% confidence intervals (Wilson score method) are reported in the text for the principal findings. *Rounding of source counts (11+21 = 32 of 33 specimens; one case unclassified). Ki-67 proliferation index (spleen): 16.21 ± 1.06% (M±SD).

These observations are consistent with the concept of sepsis-induced immunoparalysis described in the critical care literature, in which an initial hyperinflammatory phase is followed, within days, by profound depletion of lymphocyte pools and impaired antigen-dependent immune competence [3–5,9]. The discordance we observed between the two organs' macrophage responses — pronounced CD68 hyperplasia in lymph nodes (81.8%) versus a comparatively slower, siderophage-dominated response in the spleen (65.6% moderate positivity) — suggests that the lymph nodes, as the first anatomical drainage barrier of the peritoneal cavity, mount an earlier and more intense local phagocytic reaction, while splenic clearance of circulating toxic metabolites and damaged erythrocytes lags behind during the same time window. This temporal and spatial asynchrony may have direct clinical relevance for the timing of adjunctive lymphotropic and immunocorrective therapies, as has been proposed in the surgical intensive-care literature [6–8].

The severe reduction of CD20-positive B-lymphocytes (negative in 63.6% of lymph node specimens) and the near-complete loss of the organized germinal-center architecture support the hypothesis that humoral immune competence is disproportionately compromised relative to residual macrophage-mediated innate defenses in the acute phase of peritonitis. Combined with the marked CD3/CD4 T-cell depletion, these findings are compatible with the clinical observation that severe peritonitis predisposes to secondary (nosocomial) infection and septic complications even after successful source control of the primary abdominal process.

Several limitations should be acknowledged. First, the semi-quantitative grading of IHC positivity, while reproducible between the two independent observers in this study, would benefit from digital image-analysis quantification (e.g., positive-cell density per mm^2) in future work. Second, formal statistical comparison against the non-septic control cohort — including morphometric measurements of follicular and paracortical area — is the subject of the authors' ongoing dissertation research and will be reported in a dedicated comparative communication. Third, as an autopsy-based study, the findings necessarily represent the most severe (fatal) end of the clinical spectrum of peritonitis and may not directly generalize to non-fatal or successfully treated cases.

Notwithstanding these limitations, the present data provide, to our knowledge, one of the first integrated morphological and immunohistochemical descriptions of combined mesenteric lymph node and splenic collapse in adult acute secondary peritonitis, and offer a structural basis for the secondary immunodeficiency that underlies much of the excess mortality associated with this condition.

Conclusions

Acute secondary peritonitis is associated with a rapid and reproducible pattern of morphological and immunophenotypic collapse in both mesenteric lymph nodes and the spleen, characterized in lymph nodes by depletion of CD3/CD4 T-lymphocytes and CD20 B-lymphocytes with compensatory CD68 macrophage hyperplasia, and in the spleen by CD8 T-lymphocyte depletion, a parallel CD68 macrophage response, and a modest Ki-67-based proliferative response (16.21 ± 1.06%) that is insufficient to offset lymphocyte loss. These findings define a morphological substrate for the

secondary immunodeficiency observed clinically in severe peritonitis and identify lymphotropic and immunocorrective adjunctive strategies as a promising direction warranting evaluation in future prospective clinical studies, rather than a therapeutic recommendation supported by the present observational autopsy data.

Authors' contribution

A.Q.K.: study concept and design, material collection, histological and immunohistochemical analysis, manuscript drafting. E.A.E.: scientific supervision, pathological anatomy consultation, critical revision of the manuscript. Both authors read and approved the final version.

Funding source

This research did not receive external funding.

Ethics approval

The study protocol was reviewed and approved by the scientific and ethics committee of the Fergana Medical Institute of Public Health (protocol No. K/2025 0BB1, December 2025). All autopsy material was anonymized prior to analysis; the study used archival post-mortem tissue in accordance with institutional policy and the ethical principles of the Declaration of Helsinki.

Consent for publication.

This research conducted according to ethical approval of both affiliations.

Data Availability Statement

The datasets generated and analyzed during the current study are available from the corresponding author upon reasonable request.

Acknowledgments

The authors gratefully acknowledge the Republican Pathological Anatomy Center (https://www.rpam.uz/) and its Fergana branch for providing autopsy materials, histological processing facilities, and technical support essential to this study.

Conflict of interest

The authors declare no conflicts of interest.

Abbreviations

H&E	hematoxylin-eosin staining
DAB	3,3′-diaminobenzidine chromogen
IHC	immunohistochemistry
MALT	gut-associated lymphoid tissue

References

[1] Sartelli M, Catena F, Abu-Zidan FM, et al. Management of intra-abdominal infections: recommendations by the WSES 2016 consensus conference. World J Emerg Surg. 2017;12:22. https://doi.org/10.1186/s13017-017-0132-7.

[2] Singer M, Deutschman CS, Seymour CW, et al. The Third International Consensus Definitions for Sepsis and Septic Shock (Sepsis-3). JAMA. 2016;315(8):801-810. https://doi.org/10.1001/jama.2016.0287.

[3] Hotchkiss RS, Swanson PE, Freeman BD, et al. Apoptotic cell death in patients with sepsis, shock, and multiple organ dysfunction. Crit Care Med. 1999;27(7):1230-1251. https://doi.org/10.1097/00003246-199907000-00002.

[4] Hotchkiss RS, Monneret G, Payen D. Sepsis-induced immunosuppression: from cellular dysfunctions to immunotherapy. Nat Rev Immunol. 2013;13(12):862-874. https://doi.org/10.1038/nri3552.

[5] Felmet KA, Hall MW, Clark RSB, Jaffe R, Carcillo JA. Prolonged lymphopenia, lymphoid depletion, and hypoprolactinemia in children with nosocomial sepsis and multiple organ failure. J Immunol. 2005;174(6):3765-3772. https://doi.org/10.4049/jimmunol.174.6.3765.

[6] De Waele JJ. Intra-abdominal hypertension and abdominal compartment syndrome. Curr Opin Crit Care. 2022;28(6):695-701. https://doi.org/10.1097/MCC.0000000000000991.

[7] Di Franco S, Alfieri A, Fiore M, et al. A literature overview of secondary peritonitis due to carbapenem-resistant Enterobacterales (CRE) in intensive care unit (ICU) patients. Antibiotics (Basel). 2022;11(10):1347. https://doi.org/10.3390/antibiotics11101347.

[8] De Simone B, Coccolini F, Catena F, et al. Benefits of WSES guidelines application for the management of intra-abdominal infections. World J Emerg Surg. 2015;10:18. https://doi.org/10.1186/s13017-015-0013-x.

[9] Pei F, Gu B, Miao SM, Guan XD, Wu JF. Clinical practice of sepsis-induced immunosuppression: Current immunotherapy and future options. Chin J Traumatol. 2023;27(2):63-70. https://doi.org/10.1016/j.cjtee.2023.11.001.